Studies in Fungi

ARTICLE

Open Access

https://doi.org/10.48130/sif-0026-0015

Studies in Fungi **2026**, 11: e018

Adaptive responses of marine-derived *Aspergillus terreus* to salinity and chromium stress analysed by peptide mass fingerprinting

Nikita P. Lotlikar[1,2] and Samir R. Damare[1*]

[1] *Biological Oceanography Division, CSIR-National Institute of Oceanography, Dona Paula, Goa 403004, India*
[2] *School of Earth, Ocean and Atmospheric Sciences, Goa University, Taleigao, Goa 403206, India*
* Correspondence: samirdamare@gmail.com; samir.nio@csir.res.in (Damare SR)

Abstract

Fungi inhabiting marine environments often exhibit physiological and biochemical traits that enable survival in saline conditions, distinguishing them from many terrestrial counterparts. The presence of soluble osmolytes, affinity for sodium ions, and streamlined genomes aid marine biota to survive hypertonic environments. With the rise in anthropogenic activities, marine biota face multiple stresses that demand immediate acclimation and adaptation. This study evaluated the cellular responses of a marine-derived fungal isolate to variable salinities and Cr^{+6} concentrations using peptide mass fingerprinting on an LC-MS-MS QToF. The whole-cell proteins were extracted and digested with trypsin. A total of 659 proteins across nine variable conditions, including salinity (0, 35, 100 PSU) and Cr^{+6} (0, 100, 500 mg/L), were detected. Fifty-three housekeeping proteins were expressed across all conditions, categorised into carbohydrate metabolism, nucleotide metabolism, genetic information processing, and cellular processes using KEGG pathways. Variation in salinity led to the expression of proteins associated with DNA damage control and Reactive Oxygen Species (ROS) scavenging mechanisms, whereas an increase in Cr^{+6} concentration triggered the expression of proteins involved in enzymatic reduction and in transport/metal efflux. Thioredoxin expression was upregulated with fold change values of 5.011 and 5.032 at 100, and 500 mg/L Cr^{+6} at 35 PSU, and 2.358 and 1.839 at the same Cr^{+6} concentrations at 100 PSU. This indicated that upregulation of ROS-scavenging proteins was the predominant mechanism used by *A. terreus* under elevated Cr^{+6} and salt concentrations. This study observed the expression of multiple stress tolerance mechanisms to combat the synergistic effects of salt and Cr^{+6}.

Citation: Lotlikar NP, Damare SR. 2026. Adaptive responses of marine-derived *Aspergillus terreus* to salinity and chromium stress analysed by peptide mass fingerprinting. *Studies in Fungi* 11: e018 https://doi.org/10.48130/sif-0026-0015

Introduction

Industrialisation and infrastructure development require extensive extraction and use of heavy metals, generating large volumes of waste that often enter the environment. Heavy metal pollution remains a pressing concern due to its severe effects on human health and the lack of sustainable remediation solutions. Among these, chromium is one of the most carcinogenic metals, widely used in tanneries, steel/electroplating industries, and the textile industry[1,2]. Over the past 30 years, nearly 30,000 tons has been released into the environment globally[3]. In its hexavalent form, chromium mimics the sulphate oxyanion, allowing easy transmembrane transport into prokaryotic and eukaryotic cells. Once inside, it is reduced to the trivalent form, generating reactive oxygen species (ROS) that induce lipid peroxidation, DNA damage, and protein degradation[2,4,5]. Despite extensive documentation of chromium contamination in industrial effluents, the persistent toxicity of hexavalent chromium (Cr^{+6}) remains a major unresolved environmental and public health challenge. While conventional physical and chemical methods can partially mitigate heavy metal contamination, these technologies fail to remove residual Cr^{+6}, especially in saline wastewaters. This gap underscores the urgent need for eco-friendly biological strategies that can function under high ionic stress.

Marine-derived fungi have emerged as promising candidates for bioremediation in saline and metal-polluted environments. Unlike many terrestrial microbes, they exhibit inherent halotolerance, osmotic adjustment via compatible solutes (e.g., glycerol and trehalose), halophilic enzymes, and robust ion-transport systems[6,7]. These adaptations allow survival in hypersaline and alkaline habitats where conventional remediation agents fail. Several genera, including *Aspergillus*, *Penicillium*, and *Fusarium*, have demonstrated the ability to take up heavy metals, biosorb them, and enzymatically detoxify them under saline conditions[6,8]. Their ability to couple extracellular mechanisms (biosorption, bioleaching, precipitation) with intracellular strategies (enzymatic Cr^{+6} reduction, vacuolar sequestration, metallothionein production) makes them ideal candidates for sustainable wastewater treatment[7–9].

Salinity levels in contaminated habitats can vary widely, and hypersaline conditions (> 100 PSU) are encountered in evaporation ponds, tannery discharge sites, and industrial brines[9,10]. In this study, a salinity of 100 PSU was used to represent such extreme ionic environments, thereby enabling assessment of fungal performance in scenarios where conventional bioremediation agents would be ineffective. Cr^{+6} was chosen as the test metal because of its toxicity challenge posed for detoxification studies. The isolate *Aspergillus terreus* (NCBI accession no. KT956259) was selected based on preliminary screening that revealed exceptional Cr^{+6} tolerance (up to 750 mg/L) and removal efficiency (13 mg Cr g^{-1} biomass at 300 mg/L). Its marine origin suggests inherent halotolerance, and prior scanning electron microscopy (SEM) imaging and diphenylcarbazide assays indicated that both biosorption and enzymatic reduction are primary survival strategies. These features make it an ideal candidate for exploring molecular adaptations under simultaneous salt and metal stresses. *Aspergillus niger* and *Aspergillus terreus* have been reported to have potential mycoremediative capabilities for Cd^{2+} removal[11]. ESI-LCMS analysis of the crude extract of *A. terreus* revealed the expression of two new lumazine-containing peptides with pharmacological activities, thereby promoting this species for multiple applications[12]. These studies collectively strengthen the ecological and biotechnological significance of *A. terreus* and

support it as a candidate organism for remediation-driven research. At the cellular level, tolerance to heavy metals and salinity is mediated by a suite of stress-responsive proteins. Transporter families such as ATP-binding cassette (ABC) transporters, cation diffusion facilitators (CDF), and P-type ATPases play central roles in metal efflux and compartmentation[13,14]. Redox regulators, including thioredoxin and glutathione reductase, along with antioxidant enzymes such as catalases and peroxidases mitigate ROS toxicity[15,16]. Heat shock proteins and T-complex proteins further assist in protein folding and stabilization under stress[17].

Despite increasing recognition of fungal tolerance to heavy metals and salinity, most studies have examined these stressors in isolation, primarily using physiological assays or targeted biochemical measurements[15–18]. In contrast, saline industrial effluents typically impose concurrent ionic and metal stress, creating synergistic cellular pressures that cannot be predicted from single-factor experiments[9,10]. Although proteomic analyses have been conducted in selected terrestrial or clinical fungi[19,20], the integrated molecular responses of marine-derived filamentous fungi under combined stress remain poorly understood. In particular, *Aspergillus terreus*, a species noted for environmental resilience and biotechnological potential[21–23], has not been systematically investigated at the global proteome level under simultaneous salinity and chromium exposure. To address this gap, we employed LC-MS/MS-based peptide mass fingerprinting to profile whole-cell protein expression across nine salt-metal regimes. This systems-level strategy reveals coordinated stress-response pathways, metabolic prioritisation, and adaptive survival mechanisms that cannot be inferred from conventional growth or enzymatic assays, thereby providing a new mechanistic insight into fungal adaptation to complex environmental stressors. Accordingly, this study aimed to: (1) characterise the proteomic response of *A. terreus* under individual and combined Cr^{+6} and salinity stresses, (2) identify key tolerance pathways involving ROS detoxification, ion homeostasis, and metal reduction, and (3) evaluate the expression of housekeeping proteins under multi-stress exposure to gain insights into metabolic prioritisation.

Materials and methods

Strain isolation

Aspergillus terreus, #NIOSN-SK56-S52, is a previously isolated culture from Arabian Sea sediments, identified using molecular techniques (NCBI accession no. KT956259), and has been previously reported for chromium tolerance[8].

Extraction of proteins

Non-sporulated crushed mycelia of previously grown culture #NIOSN-SK56-S52 were inoculated in Czapek Dox Broth (CDB) with varying concentrations of Cr^{+6} (0, 100, and 500 mg/L), each prepared with salt solutions of 0, 35, and 100 PSU, in triplicate. The nine different metal-salt combinations were incubated at 80 rpm at 28 °C for 1 week, following which the contents were filtered, lyophilised, weighed, and processed for protein extraction. A previously standardised 3-buffer extraction method[24] was used to extract proteins from a fixed biomass quantity (30 mg). Briefly, the biomass was subjected to buffer I (Tris–$MgCl_2$, pH 8.3, 0.5 M Tris–HCl, 2% CHAPS, 20 mM $MgCl_2$, 2% DTT); buffer II (9 M urea, 4% CHAPS, 100 mM DTT—prepared in 40 mM Tris–HCl, pH 8.0); and buffer 3 (6 M urea, 3 M thiourea, 4% CHAPS, 100 mM DTT—prepared in 40 mM Tris–HCl, pH 8.0). The samples were homogenised at 6.5 m/s for 45 s after each buffer addition and centrifuged to separate the fractions. All three fractions were mixed, and the extracted proteins were quantified using the standard Folin's method and analyzed by SDS-PAGE to assess quality before proceeding with MS analysis.

Tryptic digestion and LC-MS separation

Prior to MS analysis, the protein extracts were processed for In-solution digestion using trypsin (protocol modified from Kinter & Sherman[25]). The extract was initially precipitated with HPLC-grade methanol, vacuum-dried, and suspended in urea to facilitate dissolution. Subsequently, the protein samples were reduced using dithiothreitol (DTT) and further alkylated with Iodoacetamide (IAA). The samples were digested using trypsin and analysed using the LC-MS QToF facility (6538 UHD Accurate Mass QTOF LC/MS, Agilent Technologies, USA). Digested protein samples (8 µL, four replicates) were injected in a 150 × 300 A C18 150 mm column protein chip via an autosampler. A gradient of 3%–97% across HPLC-grade acetonitrile as an organic phase, and 0.22 µm filtered and autoclaved deionised water as an aqueous phase was used to carry out LC separations over a time period of 100 min. Formic acid (0.1%) was added as an additive in both phases. An accuracy rate of 2 mg/L was maintained for the separated ions in positive mode over the range of 50–2,000 m/z. The spectral data were acquired using Mass Hunter software v5.0 (Agilent Technologies, USA) after MS/MS, and were searched in NCBI using Spectrum Mill MS Proteomics Workbench vB.04.01.141 (Agilent Technologies, USA) at 50–100 mg/L accuracy against the organism-specific database (NCBI txid 33178). Protein sequences corresponding to the differentially expressed proteins (DEPs) were retrieved from the NCBI *Aspergillus terreus* genome. The MS searches were auto-validated (false discovery rate of 1.2%), and protein summary and MPP files were generated. These files were processed in Mass Profiler Professional v14.09 (MPP13, Agilent Technologies, USA) for further analysis. Mapping and annotation steps were carried out to assign GO terms under the three ontologies: Biological Process (BP), Molecular Function (MF), and Cellular Component (CC). Differential protein abundance was calculated from MS intensity values using log 2-transformed fold changes. Multivariate differences among treatment groups were examined using Principal Component Analysis based on Euclidean distances. Statistical significance was set at $p < 0.05$.

Results

Protein profiling of *A. terreus*, #NIOSN-SK56-S52, identified 659 proteins expressed across the nine different metal-salt combinations. Based on their functional role as elucidated from KEGG pathways and metabolic processes, they were divided into 17 different categories (Fig. 1). Amino acid metabolism (41), biosynthesis of secondary metabolites (6), carbohydrate metabolism (63), cellular processes (30), energy metabolism (30), environmental information processing (38), genetic information processing (146), glycan biosynthesis and metabolism (3), lipid metabolism (12), metabolism of cofactors and vitamins (10), metabolism of other amino acids (5), metabolism of terpenoids and polyketides (4), nucleotide metabolism (16), stress response (32), xenobiotics biodegradation and metabolism (4), hypothetical proteins (213), and uncharacterised proteins (6). To further understand the contribution of proteins under each functional process under salinity stress, proteins expressed only under 0, 35, and 100 PSU were analysed (Fig. 2). Most proteins expressed at 100 PSU belonged to carbohydrate metabolism, genetic information processing, and hypothetical proteins.

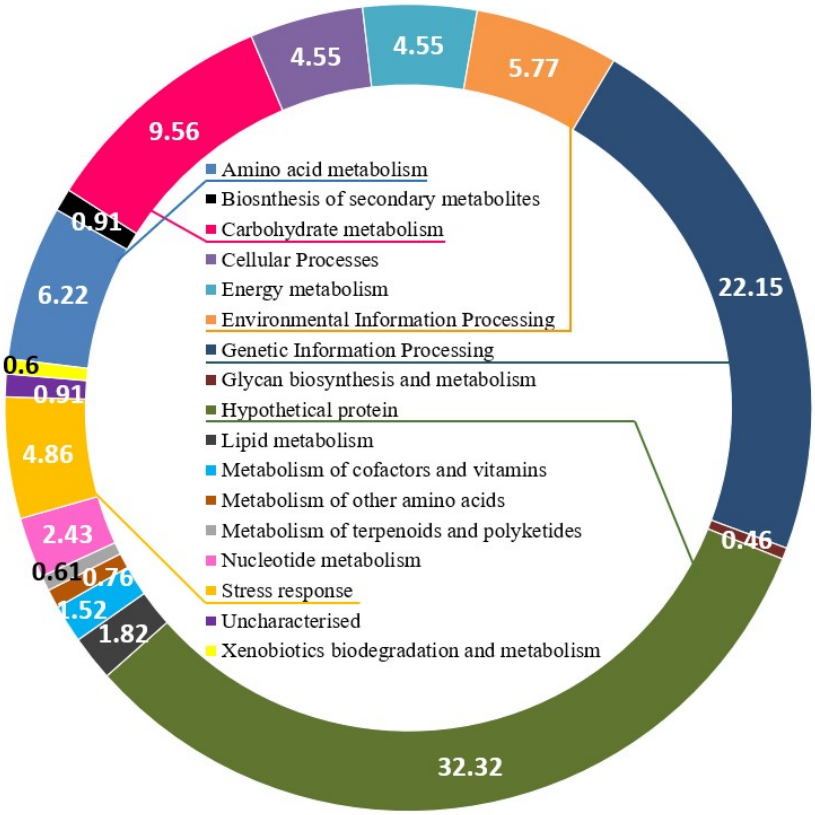

Fig. 1 Graphical representation of all proteins expressed by *A. terreus* (#NIOSN-SK56-S52) %.

Amongst the expressed proteins, 53 were commonly expressed across all nine conditions, suggesting they are involved in housekeeping metabolic activities (Table 1). Amongst these, 16 proteins (cytochrome c oxidase polypeptide IV (NCBI gi–114188084), cytochrome c oxidase polypeptide VI (NCBI gi–114188679), enolase (NCBI gi–114194476), eukaryotic initiation factor 4A (NCBI gi–114196711), Glucose-6-phosphate isomerase (NCBI gi–114193156), glyceraldehyde-3-phosphate dehydrogenase (NCBI gi–540849772), heat shock 70 kDa protein (NCBI gi–114187927), histone H2A (NCBI gi–114189434), histone H2B (NCBI gi–114189435), malate dehydrogenase (NCBI gi–114191202), phosphoglycerate kinase (NCBI gi–114197170), pyruvate kinase (NCBI gi–114193787), thioredoxin (NCBI gi–114190288), transaldolase (NCBI gi–114191388), transketolase 1 (NCBI gi–114197498), and tubulin beta chain (NCBI gi–114197233) have been previously reported as housekeeping genes in humans. In a separate study, reference genes in filamentous fungi suitable for RT-qPCR were studied and revealed nine such novel genes, namely, the β-actin, 18S rRNA, cyclophilin, histone H3, glyceraldehyde-3-phosphate dehydrogenase, α, $\beta 1$, $\beta 2$-tubulin, and ubiquitin.

A group of unique proteins expressed under specific conditions was also studied (Table 2). At 0 PSU, expression of proteins involved in biosynthetic pathways and genetic information processing was dominant, indicating a relatively stress-free physiological state consistent with the facultative marine nature of the isolate. In the presence of 500 mg/L of Cr^{+6}, proteins such as WD-repeat protein mip1 (NCBI gi–114191519), involved in cell senescence, and nonhistone chromosomal protein 6A (NCBI gi–114193442), which is involved in replication and repair were expressed. In addition to Cr^{+6} stress in the presence of 35 PSU, magnesium transporter MRS2 (NCBI gi–114190882) and T-Complex protein one subunit delta (NCBI gi–114193665) were also expressed.

The protein regulation of *A. terreus* subjected to salinity and chromium stresses was analysed using MPP software (v14.09), and the up-/downregulated proteins are shown in Table 3. It was observed that proteins commonly expressed across all conditions were generally downregulated under metal stress at all salinities, except for a few, suggesting that stress affects the expression of housekeeping genes. The priority of organisms is survival, rather than growth and reproduction, leading to downregulation of these proteins. Oxidoreductive proteins, such as cytochrome c oxidase (NCBI gi–114188084), were found to be upregulated at both 35 and 100 PSU in the presence of $Cr^{+6,}$ along with heat shock protein 82 (NCBI gi–114187927). The DNA damage checkpoint protein Rad24 (NCBI gi–114188055), involved in checkpoint response and DNA double-strand break repair was also found to be upregulated. Thioredoxin (NCBI gi–114190288), which is known to scavenge ROS actively, was upregulated at all salinities with chromium stress, with a fold change value of 5.011 and 5.532 at 100 and 500 mg/L Cr^{+6} under 35 PSU salinity, respectively. The catalase B precursor (NCBI gi–114190039) was downregulated at 35 PSU under Cr^{+6} stress. Antioxidant enzymes can be affected by free radical regeneration, and the expression of common housekeeping genes may also be altered. The downregulation of carbohydrate metabolism proteins indicated this: pyruvate kinase (NCBI gi–114193787) and transketolase 1 (NCBI gi–114197498) at 0 and 100 PSU, respectively, when subjected to Cr^{+6}.

Discussion

This study provides an in-depth mechanistic insight into how a marine-derived *Aspergillus terreus* isolate responds to simultaneous

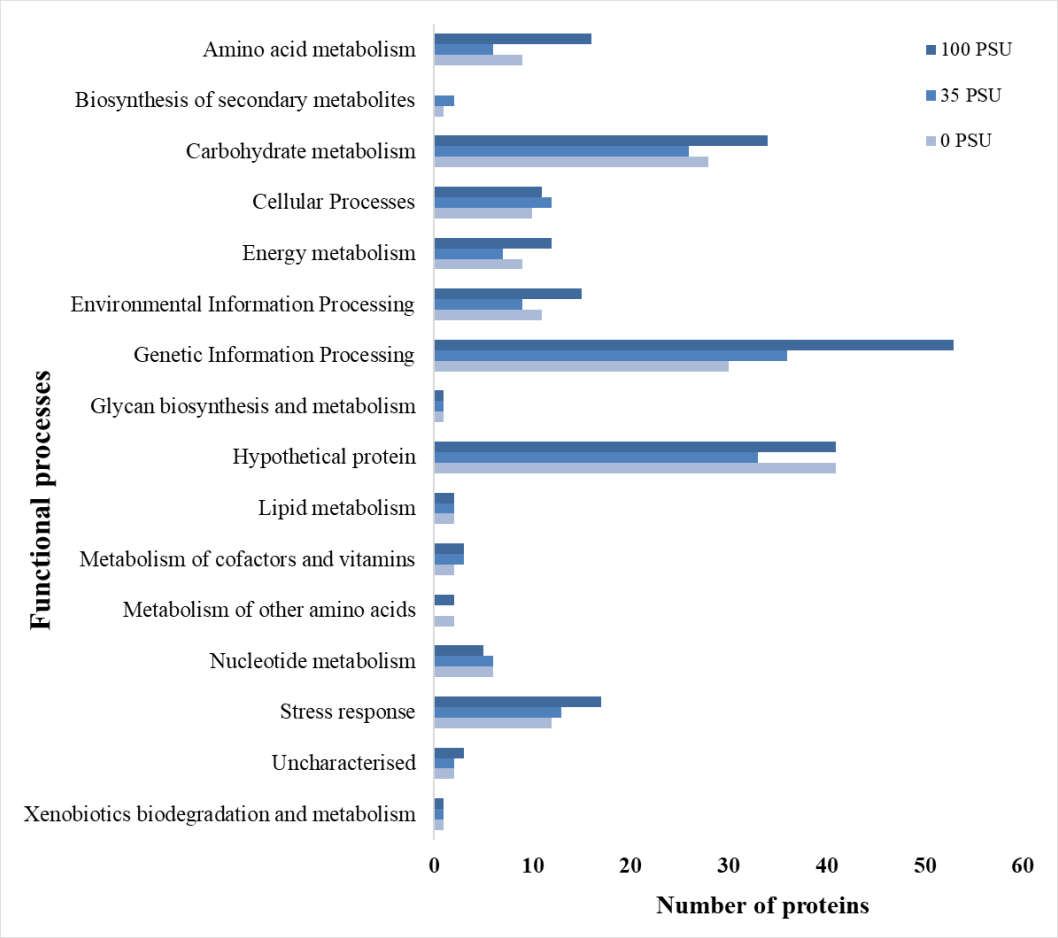

Fig. 2 Distribution of proteins expressed by *A. terreus* (#NIOSN-SK56-S52) under 0, 35, and 100 PSU salinity.

hypersaline (100 PSU) and Cr^{+6} stress—conditions that mimic industrial effluents from tanneries, electroplating, and salt-production sites where heavy metals and high ionic strength co-occur. Cr^{+6} is recognised for its high mobility, toxicity, and ability to induce oxidative and genotoxic stress, while hypersalinity creates osmotic and ionic stress that impairs many traditional bioremediation microbes.

Metal tolerance in *A. terreus* has been extensively explored and well cited[26,27]. When subjected to multi-metal stress, *Aspergillus fumigatus* PD-18, isolated from polluted banks of the Yamuna River, India expressed about 2,190 proteins, of which 387 were exclusively present under stressed conditions[19]. In another study, 2,646 proteins were identified in *Aspergillus ochraceus* grown on 20 and 70 g/L NaCl substrates, resulting in elevated ergosterol production[9]. In our study, we have shown a synergistic effect of hypersalinity and heavy metal stress on *A. terreus*.

Survival mechanisms in fungi are broadly categorised as extracellular mechanisms involving biosorption, bioleaching, biotransformation, and bioprecipitation, and intracellular mechanisms where enzymatic transformation, chelation, and multiple signalling pathways play a very important role, along with transporter proteins[27]. The most prominent transporters identified in fungi are reported to be ATP-binding cassette (ABC) transporters, conjugated ABC transporters (CT), cation diffusion transporters (CDF), MIT family (Cor A metal ion transporters), SIT (siderophore ion transport) subfamily under major facilitator superfamily (MFS), mitochondrial carriers, P-type ATPases, and Nramp family transporters[9,28]. Some of these were identified in the present study too (Table 2, Fig. 2). MacDiarmid & Gardner[14] reported aluminium tolerance in *Saccharomyces cerevisiae* due to overexpression of Mg transporters (ALR1/ALR2). In another study, Mg transporters conferred resistance to Co^{+2} growth inhibition in *Salmonella typhimurium*[29].

Fungi in the marine environment initially need to adapt to high osmotic pressure and then devise mechanisms to tolerate any metal stress. Salinity stress alone (100 PSU) caused the expression of some of the very important proteins, such as the 3-hydroxy-3-methylglutaryl-coenzyme A (HMG-CoA) reductase, a key enzyme in the mevalonate pathway and sterol biosynthesis[17], as reported in this study. *Aspergillus terreus* (NTOU4989) isolated from a Kueishan Island hydrothermal vent showed upregulation of glycerol lipid metabolism, mitogen-activated protein kinase, and pyrroline-5-carboxylate dehydrogenase genes in the presence of salt[21]. Another study reported overexpression of specific alkaloids in *A. terreus*, an endophyte isolated from *Porites pukoensis*, Xuwen coral reef, China, in the presence of 10% salt in PDB, known to modulate cell membranes and regulate membrane fluidity[22]. Interestingly, the endophytic fungus *A. terreus* isolated from the roots of *Chenopodium album* (wheat) under saline conditions showed low activities of ascorbate, catalase, and peroxidase[23]. Collectively, these three studies demonstrated that diverse *A. terreus* strains modulate both primary and secondary metabolism under salinity stress, regardless of ecological origin. Transcriptional activation of osmoadaptive pathways and alkaloid biosynthesis demonstrates the multi-faceted influence of salinity on metabolic output and stress physiology in fungi. The synergistic effect of salinity and Cr^{+6} stress led to four major stress response-related mechanisms in the current study (Fig. 3).

Table 1. Commonly expressed proteins across all salinities and Cr (VI) concentrations by *A. terreus*.

Protein name	NCBI gi	Function	Protein name	NCBI gi	Function
40S ribosomal protein S0	114194180	Translation	Hexokinase	114191625	Glycolysis/gluconeogenesis
6-phosphogluconate dehydrogenase	114191912	Pentose phosphate pathway	Histone H2A	114189434	Pyrimidine metabolism
Adenosylhomocysteinase	114197109	Cysteine and methionine metabolism	Histone H2B	114189435	Pyrimidine metabolism
ADP, ATP carrier protein	114194661	Mitochondrial biogenesis	Inorganic pyrophosphatase	114196689	Oxidative phosphorylation
Alcohol dehydrogenase I	114188844	Glycolysis/gluconeogenesis	Ketol-acid reductoisomerase, mp	114195083	Valine, leucine and isoleucine biosynthesis
Aldehyde dehydrogenase	114192389	Ascorbate and aldarate metabolism	L-xylulose reductase	114195667	Pentose and glucuronate interconversions
ATP synthase alpha chain, mp	114193514	Oxidative phosphorylation	Malate dehydrogenase, mp	114191202	Carbohydrate metabolism
ATP synthase beta chain, mitochondrial precursor	114190171	Oxidative phosphorylation	Mitochondrial peroxiredoxin PRX1	114192711	Glutathione metabolism/ stress response
ATP-citrate synthase subunit 1	114195637	Citrate cycle (TCA cycle)	Mitochondrial phosphate carrier protein	114197783	Pantothenate and CoA biosynthesis
Bacterial hemoglobin	114195409	Uncharacterised	Mitochondrial processing peptidase beta subunit	114197569	Folding, sorting and degradation
Cell division cycle protein 48	114187782	Meiosis	Nucleoside diphosphate kinase	114189539	Purine metabolism
Cerevisin precursor	114191390	Autophagy	Outer mitochondrial membrane protein porin	114192911	Mitochondrial biogenesis
Citrate synthase, mp	114189463	Citrate cycle (TCA cycle)	Phosphoglycerate kinase	114197170	Glycolysis/gluconeogenesis
Cytochrome c oxidase polypeptide IV, mp	114188084	Oxidative phosphorylation	Pyruvate decarboxylase	114193380	Glycolysis/gluconeogenesis
Cytochrome c oxidase polypeptide VI, mp	114188679	Oxidative phosphorylation	Pyruvate kinase	114193787	Glycolysis/gluconeogenesis
DNA damage checkpoint protein rad24	114188055	Stress/ DNA repair	S-adenosylmethionine synthetase	114197201	Cysteine and methionine metabolism
Elongation factor 1-beta	114197267	Translation	Superoxide dismutase, mp	114191387	Response to oxidative stress
Elongation factor 2	114196384	Translation	Thioredoxin	114190288	Response to oxidative stress
Enolase	114194476	Glycolysis / Gluconeogenesis	Transaldolase	114191388	Carbohydrate metabolism
Eukaryotic initiation factor 4A	114196711	Translation	Transketolase 1	114197498	Carbohydrate metabolism
Eukaryotic translation initiation factor 5A	114193909	Translation	Triosephosphate isomerase	114192224	Carbohydrate metabolism
Glucose-6-phosphate isomerase	114193156	Carbohydrate metabolic process	Tubulin alpha-1 chain	114193585	Transport and catabolism
Glyceraldehyde-3-phosphate dehydrogenase	540849772	Carbohydrate metabolic process	Tubulin beta chain	114197233	Transport and catabolism
GTP-binding nuclear protein GSP1/Ran	114194939	Signal transduction	UDP-glucose 4-epimerase	114190193	Carbohydrate metabolism
Heat shock 70 kDa protein	114187927	Stress response	Vacuolar protease A precursor	114193423	Fungal-type cell wall organization
Heat shock protein 82	114189469	Stress response	Woronin body major protein	114191425	Translation
Heat shock protein SSC1, mp	114193179	Stress response			

mp = mitochondrial precursor.

Sodium ions, which are themselves toxic, act as signalling molecules to open up non-selective cation channels within the cell membrane, causing activation of Ca^{+2} transporters, MAPK pathways, ROS generation, and activation of subsequent repair mechanisms such as SOS repair and production of NADPH oxidase[30] HMG-CoA, also identified as the biochemical signature of halophily, is reportedly involved in post-translational modification by prenylation in *H. werneckii* and catering to metabolic demands under hypo-, hypersaline conditions[31]. Protein kinases, a group of silent stress busters, are widely reported and cited in eukaryotic systems for regulatory roles in managing stress response[32]. Expression of proteins involved in signalling, regulation, or the promotion of protein kinase production is indicative of stressful conditions. Almeida-Dalmet et al.[33] reported upregulated expression of the protein kinase gene and phenyl acetyl CoA ligase gene under salinity and temperature stresses in the *Haloarcula* strain.

ROS-generated stress leads to the production of proteins such as kinases and phosphatases, which may be grouped as salt stress proteins that further enhance the production of proteins involved in cell wall building, nutrient metabolism, carbohydrate metabolism, and cell enlargement and division[34]. Both enzymatic (catalase, superoxide dismutase, peroxidases, glutathione reductases) and non-enzymatic (ascorbic acid, glutathione, phenolics, proline) antioxidants have immense ability to scavenge ROS[18]. Ankyrin repeats have also been reported to participate in ROS under salt stress[35]. Some of these proteins were expressed under salinity stress in the current study (Tables 1, 2). Proteins such as thioredoxin, catalase, superoxide dismutase, and glutathione S-transferase, along with heat shock proteins have been previously reported in the opportunistic pathogen, *A. terreus,* when subjected to 37 °C for 48 h and exposed to amphotericin B[20]. Toxicity of metal, once within the cell, can be curbed using multiple measures, one of which is organelle compartmentation or vacuolar accumulation after being chelated using glutathione, metallothioneins, or phytochelatins, as in the case of hyperaccumulating plants[36,37]. Expression of these T-complex proteins (TCPs) has been reported to be dominant under salt stress, along with heat shock proteins[38], and was detected under 35 and 100 PSU salt stress in the current study. Elevated salt concentrations may cause physiological changes in subjected organisms and trigger molecular, cellular, and metabolic responses. Expression of stress proteins, proteins involved in oxidative phosphorylation, and transporter proteins was observed under Cr^{+6} stress and increasing salinity, indicating a synergistic effect of both stresses on the culture.

Table 2. Unique proteins expressed at varying salinities and Cr (VI) concentrations and combinations by *A. terreus*.

Condition	Protein name	NCBI gi	Function
0 PSU, 0 mg/L	ATP-dependent RNA helicase DOB1	114192864	Spliceosome
	Cystathionine beta-lyase	114195508	Cysteine and methionine metabolism
	Glycolipid-anchored surface protein 5 precursor	114189622	Glycan biosynthesis and metabolism
	Guanine nucleotide-binding protein beta subunit	114195314	Transport and catabolism
	Methylcrotonoyl-CoA carboxylase beta chain, mitochondrial precursor	114191417	Valine, leucine, and isoleucine degradation
	Molybdenum cofactor biosynthesis protein 1 B	114192533	Folding, sorting, and degradation
	Vacuolar ATP synthase subunit B	114196357	Autophagy
0 PSU, 100 mg/L	Allergen Asp f 7	114192930	TNF signaling pathway
	Alternative oxidase, mitochondrial precursor	114190002	Oxidative phosphorylation
	Arabinan endo-1,5-alpha-L-arabinosidase A precursor	114193790	carbohydrate metabolic process
	ATP-dependent protease La	114196169	Cell growth and death
	DNA-directed RNA polymerase II 45 kDa polypeptide	114196335	Transcription
	Quinate permease	114190347	Quinate metabolism
0 PSU, 500 mg/L	Anthranilate synthase component II	114197450	Phenylalanine, tyrosine, and tryptophan biosynthesis
	Endochitinase 1 precursor	114194948	Starch and sucrose metabolism
	Glycerol-3-phosphate dehydrogenase, mitochondrial precursor	114193625	carbohydrate metabolic process
	Nonhistone chromosomal protein 6A	114193442	Replication and repair
	Orotate phosphoribosyltransferase	114196505	Pyrimidine metabolism
	Proliferating cell nuclear antigen	114195863	DNA replication
	Serine/threonine-protein phosphatase 2A 56 kDa regulatory subunit delta 1 isoform	114188660	Cell cycle
	Signal recognition particle 54 kDa protein	114189491	Folding, sorting, and degradation
	Transcriptional repressor rco-1	114191721	Transcription
	Vacuolar ATP synthase subunit E	114190926	Oxidative phosphorylation
	WD-repeat protein mip1	114190613	cellular senescence
35 PSU, 0 mg/L	26S proteasome regulatory subunit rpn-1	114195360	Proteosome
	3-methyl-2-oxobutanoate hydroxymethyltransferase	114191519	Pantothenate and CoA biosynthesis
	Alpha,alpha-trehalose-phosphate synthase 1	114194901	Starch and sucrose metabolism
	Catalase	114196544	Stress response
	cell differentiation protein rcd1	114194699	Meiosis
	Chromosome segregation protein sudA	114196456	Meiosis
	CURS1	443610053	Biosynthesis of secondary metabolites
	Nonsense-mediated mRNA decay protein 3	114194516	Translation
	Nonspecific lipid-transfer protein, mitochondrial precursor	114192954	Lipid metabolism
	Protein kinase lkh1	114192486	MAPK signaling pathway
35 PSU, 100 mg/L	1,4-alpha-glucan branching enzyme	114190170	Starch and sucrose metabolism
	Coatomer beta subunit	114197239	Oxidative phosphorylation
	Inner membrane magnesium transporter MRS2, mitochondrial precursor	114190882	Metal ion transmembrane transporter activity
	Inositol-3-phosphate synthase	114189610	phosphatidylinositol signaling system
	NADH-ubiquinone oxidoreductase 21 kDa subunit	114196031	Oxidative phosphorylation
	Pre-mRNA splicing factor CLF1	114197157	Transcription
	Zinc-regulated transporter 1	114193659	Transcription factors
35 PSU, 500 mg/L	26S protease regulatory subunit 8	114196020	Proteosome
	Activator 1 subunit 3	114188298	Folding, sorting, and degradation
	Alanyl-tRNA synthetase	114196954	Aminoacyl-tRNA biosynthesis
	C-1-tetrahydrofolate synthase, mitochondrial precursor	114196661	Folate biosynthesis
	Cholinesterase	114195928	Glycerophospholipid metabolism
	Iron sulfur assembly protein 1	114194102	Biotin metabolism
	Lactoylglutathione lyase	114191927	Pyruvate metabolism
	Methionine aminopeptidase 2B	114192909	Fructose and mannose metabolism
	NAD-dependent histone deacetylase SIR2	114193955	Metabolism of cofactors and vitamins
	Nucleolar GTP-binding protein 2	114192691	Translation
	Splicing factor 3B subunit 3	114194961	Spliceosome
	T-complex protein 1 subunit delta	114193665	Chaperones and folding catalysts
	Transcription initiation factor TFIID subunit 12	114189293	Transcription
100 PSU, 0 mg/L	3-hydroxy-3-methylglutaryl-coenzyme A reductase	114188011	Melavonate pathway/terpenoid synthesis
	Ankyrin repeat protein nuc-2	114191665	Toll and Imd signaling pathway
	Argininosuccinate lyase	114196749	Arginine biosynthesis
	Aryl-alcohol dehydrogenase	114196508	Tyrosine metabolism
	Casein kinase I isoform epsilon	114190610	Ribosome biogenesis in eukaryotes
	Chitin synthase 6	114196376	Amino sugar and nucleotide sugar metabolism
	Dual specificity tyrosine-phosphorylation regulated kinase 2	114189670	MAPK signaling pathway

(to be continued)

Table 2. (continued)

Condition	Protein name	NCBI gi	Function
100 PSU, 0 mg/L	Mannose-6-phosphate isomerase	114197475	Fructose and mannose metabolism
	Peroxisomal biogenesis factor 6	114196745	Transport and catabolism
	Proteasome subunit alpha type 1	114190652	Folding, sorting, and degradation
	Serine/threonine-protein kinase CLA4	114188881	Cell cycle
	Two-component signaling kinase TcsC	421994880	Signal transduction
	Vacuolar ATP synthase 98 kDa subunit	114194052	Oxidative phosphorylation
100 PSU, 100 mg/L	Aldo-keto reductase yakc	114195515	Arachidonic acid metabolism
	Calcium-transporting ATPase 1	114191621	Calcium signaling pathway
	Cytochrome c oxidase polypeptide V, mitochondrial precursor	114190172	Oxidative phosphorylation
	DNA repair and recombination protein RAD54	114188055	Stress/ DNA repair
	Enoyl-CoA hydratase, mitochondrial precursor	114196542	Fatty acid elongation
	G2/mitotic-specific cyclin cdc13	114195591	Cell cycle
	Glutaryl-CoA dehydrogenase, mitochondrial precursor	114189298	Lipid metabolism
	GTP-binding protein 1	114195273	Signal transduction
	Maleylacetate reductase	114193824	Chlorocyclohexane and chlorobenzene degradation
	Peroxidase/catalase 2	114189895	Stress response
	Phosphoribosylglycinamide formyltransferase	114196550	Purine metabolism
	T-complex protein 1 subunit alpha	114195604	Chaperones and folding catalysts
	Threonine synthase	114191253	Glycine, serine, and threonine metabolism
	Thymidylate synthase	114187858	Pyrimidine metabolism
100 PSU, 500 mg/L	26S proteasome non-ATPase regulatory subunit 3	114189291	Proteosome
	3-isopropylmalate dehydrogenase B	114194981	Valine, leucine, and isoleucine biosynthesis
	Aconitate hydratase, mitochondrial precursor	114194899	Citrate cycle (TCA cycle)
	Branched-chain-amino-acid aminotransferase	114191652	Cysteine and methionine metabolism
	Bystin	114193014	Ribosome biogenesis
	DNA replication licensing factor mcm7	114193195	DNA replication
	Elongation factor G	114188759	Translation
	Elongation factor G 1, mitochondrial precursor	114192760	Translation
	Eukaryotic peptide chain release factor subunit 1	114188901	Translation
	Eukaryotic translation initiation factor 2 gamma subunit	114192814	Translation
	Eukaryotic translation initiation factor 5B	114193915	Translation
	Eukaryotic translation initiation factor 6	114188867	Translation
	Exoglucanase 1 precursor	114192372	Starch and sucrose metabolism
	Glycine cleavage system H protein	114197351	Glycine, serine, and threonine metabolism
	HIRA-interacting protein 5	114193863	Oxidative phosphorylation
	Isovaleryl-CoA dehydrogenase, mitochondrial precursor	114191418	Amino acid metabolism
	Mitochondrial import receptor subunit tom-20	114192401	Transporters
	Multidrug resistance protein 1	114188861	Drug resistance
	Myosin-1	114190321	Cellular processes
	NADH-ubiquinone oxidoreductase 19.3 kDa subunit, mitochondrial precursor	114191677	Oxidative phosphorylation
	NADH-ubiquinone oxidoreductase 51 kDa subunit, mitochondrial precursor	114194075	Oxidative phosphorylation
	Nucleolar essential protein 1	114189301	Translation
	Nucleolar protein NOP58	114194165	Translation
	Phenylacrylic acid decarboxylase	114187643	Phenylpropanoid biosynthesis
	Phospho-2-dehydro-3-deoxyheptonate aldolase	114193629	Phenylalanine, tyrosine, and tryptophan biosynthesis
	Prohibitin-2	114188359	Mitochondrial biogenesis
	Queuine tRNA-ribosyltransferase	114187859	queuosine biosynthesis
	Sec14 cytosolic factor	114193260	Transporters
	Small nuclear ribonucleoprotein Sm D1	114192048	Spliceosome
	Thioredoxin reductase	114194755	Response to oxidative stress
	Tyrosyl-tRNA synthetase	114195131	Aminoacyl-tRNA biosynthesis
	Valyl-tRNA synthetase, mitochondrial precursor	114189806	Aminoacyl-tRNA biosynthesis

Housekeeping proteins are vital for survival and are expressed in organisms at all times, irrespective of favourable or stressful conditions[39]. However, their expression may be altered or become irregular under certain conditions[40]. We found changes in the expressions of some housekeeping proteins in response to the stress imparted. Glyceraldehyde-3-phosphate dehydrogenase expression was downregulated at 0 PSU salt concentration in the presence of Cr^{+6}, but was upregulated at 100 PSU (Table 3). Similarly, the expression of the Tubulin beta chain varied under different salt concentrations in the presence of metal. Differential expression of glyceraldehyde-3-phosphate dehydrogenase and beta-actin genes was also reported during the course of hepatitis C virus-induced hepatocellular carcinoma (HCV-HCC)[41]. Further, this differential expression property has previously been used to diagnose lung cancer[42]. Therefore, any drastic variations in the expression levels of such genes may shed light on an organism's adaptive strategies in the presence of stress. On the contrary, relying solely on the expression of housekeeping genes as an internal reference may not

Table 3. Protein regulation by *A. terreus* under chromium stress.

Protein name	NCBI gi	FC[a]	FC[b]	Protein name	NCBI gi	FC[a]	FC[b]
Commonly upregulated proteins at 0 PSU (17 nos.)							
40S ribosomal protein S5	114197792	2.766	0.738	Hypothetical protein ATEG_07937	114190499	1.383	0.298
ADP, ATP carrier protein	114194661	1.045	0.756	Hypothetical protein ATEG_08274	114189747	3.400	2.199
ATP synthase gamma chain, mp	114195813	2.271	3.245	Ketol-acid reductoisomerase, mp	114195083	1.382	0.463
Bacterial hemoglobin	114195409	0.313	1.337	Mitochondrial phosphate carrier protein	114197783	1.587	2.695
Dihydrolipoyllysine-residue acetyltransferase component of pyruvate dehydrogenase complex, mp	114191205	2.716	1.100	Mitochondrial processing peptidase β subunit	114197569	0.663	1.044
Hypothetical protein ATEG_04611	114193358	2.318	3.437	S-adenosylmethionine synthetase	114197201	2.128	3.614
Hypothetical protein ATEG_04814	114193561	0.792	3.772	Sulfate adenylyltransferase	114189197	2.245	1.548
Hypothetical protein ATEG_06597	114191441	2.031	1.491	Thioredoxin	114190288	1.054	1.366
Hypothetical protein ATEG_07125	114190809	3.702	4.735				
Commonly downregulated proteins at 0 PSU (28 nos.)							
30 kDa heat shock protein	114195087	−1.489	−3.989	Hypothetical protein ATEG_03766	114193868	−3.495	−4.500
40S ribosomal protein S7	114193349	−0.400	−1.867	Hypothetical protein ATEG_04029	114194131	−0.329	−5.081
Adenosylhomocysteinase	114197109	−2.504	−1.255	Hypothetical protein ATEG_07892	114190454	−2.436	−3.554
Alcohol dehydrogenase I	114188844	−1.262	−2.186	Nucleoside diphosphate kinase	114189539	−0.270	−1.198
Allergen Asp f 15 precursor	114196299	−1.670	−1.123	Peptidyl-prolyl cis-trans isomerase, mp	114188009	−1.079	−1.164
ATP-citrate synthase subunit 1	114195637	−0.241	−1.403	Phosphoglycerate kinase	114197170	−0.876	−1.691
Cell division control protein 3	114191267	−0.026	−1.425	Pyruvate decarboxylase	114193380	−1.080	−1.857
Citrate synthase, mp	114189463	−1.648	−1.952	Pyruvate kinase	114193787	−1.254	−2.345
Cytochrome c peroxidase, mp	114194980	−2.517	−2.468	Superoxide dismutase, mp	114197603	−2.990	−5.415
Enolase	114194476	−0.766	−1.167	Transaldolase	114191388	−0.240	−1.012
Eukaryotic translation initiation factor 5A	114193909	−1.433	−2.481	Transketolase 1	114197498	−2.501	−3.119
Fructose-bisphosphate aldolase	114193450	−1.280	−2.084	Triosephosphate isomerase	114192224	−2.191	−2.825
Glyceraldehyde-3-phosphate dehydrogenase	114188308	−0.692	−1.064	Tubulin beta chain	114197233	−0.815	−2.778
Histone H2A	114189434	−0.898	−1.043	UDP-glucose 4-epimerase	114190193	−0.734	−2.722
Commonly upregulated proteins at 35 PSU (63 nos.)							
2,3-bisphosphoglycerate-independent phosphoglycerate mutase	114196604	2.324	3.720	Heat shock 70 kDa protein	114187927	1.578	1.973
40S ribosomal protein S0	114194180	2.509	3.045	Heat shock protein 82	114189469	4.514	3.642
40S ribosomal protein S12	114194654	1.124	2.256	Hexokinase	114191625	2.103	1.510
40S ribosomal protein S4-A	114189168	0.829	1.918	Histone H4.2	114196427	0.609	1.157
40S ribosomal protein S5	114197792	0.692	2.155	Hypothetical protein ATEG_01302	114196359	0.892	1.508
40S ribosomal protein S7	114193349	1.349	2.410	Hypothetical protein ATEG_04182	114194284	1.632	2.166
60S ribosomal protein L13	114196001	0.697	2.429	Hypothetical protein ATEG_05472	114192841	1.102	1.171
60S ribosomal protein L14-A	114190763	1.619	1.637	Hypothetical protein ATEG_07125	114190809	0.681	1.325
60S ribosomal protein L17	114197587	0.870	1.694	Hypothetical protein ATEG_07222	114190906	1.819	1.008
60S ribosomal protein L23A	114188904	0.374	1.561	Inorganic pyrophosphatase	114196689	1.807	1.504
60S ribosomal protein L4-2	114188716	1.276	3.004	Ketol-acid reductoisomerase, mp	114195083	2.091	2.069
60S ribosomal protein L43	114187815	1.296	1.853	Malate dehydrogenase, mp	114191202	1.331	0.976
6-phosphogluconate dehydrogenase	114191912	1.563	2.096	Mitochondrial peroxiredoxin PRX1	114192711	2.872	3.131
Actin	114190657	1.288	1.599	Mitochondrial phosphate carrier protein	114197783	2.236	2.705
ADP, ATP carrier protein	114194661	0.997	1.245	Mitochondrial processing peptidase β subunit	114197569	2.160	3.326
ATP synthase alpha chain, mp	114193514	1.267	1.362	Outer mitochondrial membrane protein porin	114192911	1.732	0.165
ATP synthase beta chain, mp	114190171	1.010	1.178	Peptidyl-prolyl cis-trans isomerase cyp8	114192233	0.985	1.330
ATP-citrate synthase subunit 1	114195637	3.057	3.839	Phosphoglycerate kinase	114197170	0.272	1.118
Bacterial hemoglobin	114195409	2.965	5.151	Predicted protein	114191395	0.951	2.529
Cell division cycle protein 48	114187782	2.262	1.642	Protein MMF1, mp	114196923	1.349	0.962
Cerevisin precursor	114191390	1.711	1.105	Rab GDP-dissociation inhibitor	114196519	1.423	1.503
Conserved hypothetical protein	114196475	1.396	2.587	S-adenosylmethionine synthetase	114197201	2.622	3.822
Cytochrome c oxidase polypeptide IV, mp	114188084	3.281	3.780	Thioredoxin	114190288	5.011	5.532
Cytochrome c oxidase polypeptide VI, mp	114188679	1.105	1.648	Transaldolase	114191388	1.929	1.609
DNA damage checkpoint protein rad24	114188055	1.449	1.457	Transketolase 1	114197498	1.548	0.710
Elongation factor 1-alpha	114194584	1.020	1.685	Triosephosphate isomerase	114192224	1.975	2.215
Elongation factor 2	114196384	1.127	1.052	Tubulin beta chain	114197233	1.919	0.493
Eukaryotic initiation factor 4A	114196711	2.100	1.766	UDP-glucose 4-epimerase	114190193	2.064	1.063
Fructose-bisphosphate aldolase	114193450	0.739	1.528	Uricase	114196577	1.110	1.717
Glucose-6-phosphate isomerase	114193156	2.410	3.284	Vacuolar protease A precursor	114193423	1.442	1.539
Glyceraldehyde-3-phosphate dehydrogenase	114188308	0.718	1.222	Woronin body major protein	114191425	1.183	0.351
GTP-binding nuclear protein GSP1/Ran	114194939	2.158	2.763				
Commonly downregulated proteins at 35 PSU (02 nos.)							
Catalase B precursor	114190039	−0.738	−1.267	Hypothetical protein ATEG_04940	114192309	−1.152	−3.181

(to be continued)

Table 3. (continued)

Protein name	NCBI gi	FC[a]	FC[b]	Protein name	NCBI gi	FC[a]	FC[b]
Hypothetical protein ATEG_02219	114195481	−1.691	−0.240	Hypothetical protein ATEG_07892	114190454	−2.963	−0.709
Commonly upregulated proteins at 100 PSU (60 nos.)							
40S ribosomal protein S12	114194654	1.270	0.419	ATP synthase D chain, mp	114190764	1.467	1.799
40S ribosomal protein S14	114196585	1.452	2.090	ATP synthase gamma chain, mp	114195813	1.783	2.225
40S ribosomal protein S18	114194976	1.482	1.444	ATP synthase subunit 4, mp	114193524	1.860	1.327
40S ribosomal protein S2	114189125	1.241	1.859	Bacterial hemoglobin	114195409	1.772	2.860
40S ribosomal protein S22	114192590	2.391	3.118	Cell division cycle protein 48	114187782	0.806	2.239
40S ribosomal protein S3	114194638	2.251	1.819	Cerevisin precursor	114191390	1.431	0.988
40S ribosomal protein S4-A	114189168	1.112	2.637	Citrate synthase, mp	114189463	0.473	1.825
40S ribosomal protein S5	114197792	1.161	1.795	Conserved hypothetical protein	114196475	2.126	2.297
40S ribosomal protein S6	114194091	2.466	4.689	Cytochrome c	114196337	1.893	1.957
40S ribosomal protein S7	114193349	1.105	2.259	Cytochrome c oxidase polypeptide IV, mp	114188084	0.740	1.015
40S ribosomal protein S8-B	114193882	1.527	3.730	D-3-phosphoglycerate dehydrogenase 2	114188915	0.435	2.825
60S acidic ribosomal protein P0	114195838	1.810	2.371	Dihydrolipoyllysine-residue acetyltransferase component of pyruvate dehydrogenase complex, mp	114191205	0.997	2.215
60S ribosomal protein L10-B	114188346	0.697	1.575	Elongation factor 1-alpha	114194584	0.602	1.119
60S ribosomal protein L11	114192799	1.454	3.276	Glucose-6-phosphate 1-dehydrogenase	114196680	4.509	4.948
60S ribosomal protein L12	114195804	0.921	1.374	Heat shock protein 60, mp	114188341	1.130	2.925
60S ribosomal protein L13	114196001	1.628	1.675	Heat shock protein 82	114189469	0.437	1.829
60S ribosomal protein L14-A	114190763	0.583	1.701	Heat shock protein SSC1, mp	114193179	0.308	1.746
60S ribosomal protein L17	114197587	3.057	4.125	Hypothetical protein ATEG_03432	114195006	2.416	2.892
60S ribosomal protein L2	114188833	3.644	3.886	Hypothetical protein ATEG_03766	114193868	0.613	1.904
60S ribosomal protein L20	114193847	0.326	1.473	Hypothetical protein ATEG_04611	114193358	2.060	1.378
60S ribosomal protein L22	114194260	1.264	1.760	Hypothetical protein ATEG_08708	114189140	2.900	2.194
60S ribosomal protein L23	114188046	1.750	2.336	Hypothetical protein ATEG_09084	114188521	0.106	1.874
60S ribosomal protein L23A	114188904	1.337	2.134	Isocitrate dehydrogenase subunit 2, mp	114197413	2.411	3.027
60S ribosomal protein L27a	114189407	1.732	3.080	Mitochondrial phosphate carrier protein	114197783	0.882	2.216
60S ribosomal protein L34-B	114188081	2.250	2.919	Mitochondrial processing peptidase β subunit	114197569	1.436	2.454
60S ribosomal protein L4-2	114188716	1.634	1.888	NADH-ubiquinone oxidoreductase 30.4 kDa subunit, mp	114191474	0.895	1.475
60S ribosomal protein L43	114187815	0.561	1.072	Peptidyl-prolyl cis-trans isomerase cyp8	114192233	1.009	0.636
60S ribosomal protein L7	114195468	1.105	1.453	Pyruvate dehydrogenase E1 component α subunit, mp	114193839	1.026	1.899
ADP, ATP carrier protein	114194661	0.351	1.904	Thioredoxin	114190288	2.358	1.839
Aspartate aminotransferase, mp	114197845	0.859	1.208	Tubulin beta chain	114197233	0.194	1.720
Commonly downregulated proteins at 100 PSU (14 nos.)							
2,3-bisphosphoglycerate-independent phosphoglycerate mutase	114196604	−0.221	−1.250	Hypothetical protein ATEG_07892	114190454	−0.894	−3.342
Adenosylhomocysteinase	114197109	−1.786	−0.439	Inorganic pyrophosphatase	114196689	−0.643	−2.344
Aldehyde dehydrogenase	114192389	−1.095	−0.509	Phosphoglycerate kinase	114197170	−0.042	−1.044
Cytochrome c peroxidase, mp	114194980	−1.986	−1.345	Pyruvate kinase	114193787	−1.707	−1.342
Fructose-bisphosphate aldolase	114193450	−0.326	−1.110	Superoxide dismutase, mp	114197603	−2.076	−0.414
Glucose-6-phosphate isomerase	114193156	−1.044	−0.166	Transketolase 1	114197498	−1.322	−0.163
Hypothetical protein ATEG_03892	114193994	−1.528	−0.492	UTP--glucose-1-phosphate uridylyltransferase	114196870	−0.195	−1.299

FC[a] = fold change values for proteins expressed under chromium stress (100 ppm vs. 0 ppm); FC[b] = fold change values for proteins expressed under chromium stress (500 ppm vs. 0 ppm); mp = mitochondrial precursor.

always generate dependable results. A study by Irie et al.[43] reported that atorvastatin altered the expression of housekeeping genes, thereby misleading the data obtained for the target gene expression set, and emphasised caution when using internal reference gene expression data, especially in cancer-related studies. Such caution during experimental setup has also been reported previously[44]. Although RT-qPCR analysis of this gene expression in the current study would shed more light on this conclusion, the preliminary experiments also provide reliable proof.

Conclusions

This study shows that the marine-derived *A. terreus* employs a coordinated and multi-layered defense network to survive the combined effects of Cr^{+6} stress and hypersaline (100 PSU) conditions. Based on proteomics results, the isolate primarily activates DNA damage control and repair systems, in addition to robust ROS detoxification mechanisms, when exposed to salinity alone, thereby protecting cellular components and genomic integrity. The addition of Cr^{+6} induces further adaptive responses, such as upregulation of membrane transporters to mediate metal and ion flux and the conversion of toxic Cr^{+6} to the less harmful Cr^{+3} via enzymatic reduction pathways. Together, these systems lessen the cumulative harm and enable the cell to redistribute resources from growth to essential survival functions. The ecological adaptability of *A. terreus* and its potential for bioremediation of saline, metal-contaminated wastewaters are highlighted by its ability to continue functioning under extreme ionic and oxidative pressures, where conventional

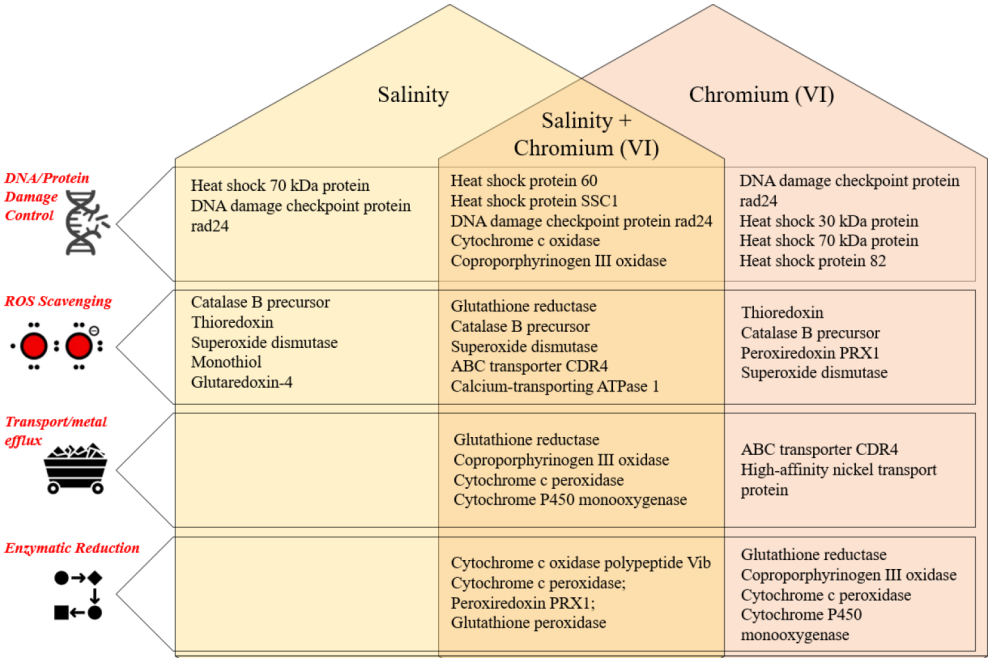

Fig. 3 Mechanism of metal tolerance by *A. terreus* (#NIOSN-SK56-S52) under salinity and chromium stress.

microorganisms are ineffective. Together, these abilities contribute to the strategic application of marine fungi for high-salinity sustainable heavy-metal remediation technologies, and enhance our knowledge of fungal stress adaptation.

Author contributions

The authors confirm their contributions to the paper as follows: conceptualised: Lotlikar NP, Damare SR; carried out as part of the doctoral thesis: Lotlikar NP. Both authors reviewed the results and approved the final version of the manuscript.

Data availability

Data will be made available on request.

Acknowledgments

The first author is thankful to the Council of Scientific and Industrial Research (CSIR) for the fellowship 18-12/2011(ii)EU-V and the Director, CSIR-NIO, for providing the facilities. Both authors are thankful to the Council of Scientific and Industrial Research (CSIR), Govt. of India, for funding this work under the project PSC0206. The first author is thankful to the Council of Scientific and Industrial Research (CSIR) for the fellowship 18-12/2011(ii)EU-V. The authors are also thankful to anonymous reviewers for their comments, which improved the manuscript.

Conflict of interest

The authors declare that they have no conflict of interest.

Dates

Received 28 May 2025; Revised 20 March 2026; Accepted 10 April 2026; Published online 16 June 2026

References

[1] Matilda CS, Mannully ST, Viditha RP, Shanthi C. 2019. Protein profiling of metal-resistant *Bacillus cereus* VITSH1. *Journal of Applied Microbiology* 127:121–133

[2] Islam S, Kamila S, Chattopadhyay A. 2022. Toxic and carcinogenic effects of hexavalent chromium in mammalian cells *in vivo* and *in vitro*: a recent update. *Journal of Environmental Science and Health, Part C* 40:282–315

[3] Zhao H, Wu Y, Lan X, Yang Y, Wu X, et al. 2022. Comprehensive assessment of harmful heavy metals in contaminated soil in order to score pollution level. *Scientific Reports* 12:3552

[4] DesMarias TL, Costa M. 2019. Mechanisms of chromium-induced toxicity. *Current Opinion in Toxicology* 14:1–7

[5] Pavesi T, Moreira JC. 2020. Mechanisms and individuality in chromium toxicity in humans. *Journal of Applied Toxicology* 40:1183–1197

[6] Hlihor RM, Roşca M, Drăgoi EN, Simion IM, Favier L, et al. 2023. New insights into the application of fungal biomass for chromium(VI) bioremoval from aqueous solutions using Design of Experiments and Differential Evolution based neural network approaches. *Chemical Engineering Research and Design* 190:233–254

[7] Yu XZ, Lin YJ, Zhang Q. 2019. Metallothioneins enhance chromium detoxification through scavenging ROS and stimulating metal chelation in *Oryza sativa*. *Chemosphere* 220:300–313

[8] Lotlikar NP, Damare SR, Meena RM, Linsy P, Mascarenhas B. 2018. Potential of marine-derived fungi to remove hexavalent chromium pollutant from culture broth. *Indian Journal of Microbiology* 58:182–192

[9] McGenity TJ, Oren A. 2012. Hypersaline environments. In *Life at Extremes: Environments, Organisms and Strategies for Survival*. UK: CABI. pp. 402–437 doi: 10.1079/9781845938147.0402

[10] Calheiros CSC, Silva G, Quitério PVB, Crispim LFC, Brix H, et al. 2012. Toxicity of high salinity tannery wastewater and effects on constructed wetland plants. *International Journal of Phytoremediation* 14:669–680

[11] Rabab AM, Asmaa ST, Asmaa HM, Shereen AS. 2025. Adaptability assessment of *Aspergillus niger* and *Aspergillus terreus* isolated from long-term municipal/industrial effluent-irrigated soils to cadmium stress. *BMC Microbiology* 25:297

[12] You M, Liao L, Hong SH, Park W, Kwon DI, et al. 2015. Lumazine peptides from the marine-derived fungus *Aspergillus terreus*. *Marine Drugs* 13:1290–1303
[13] Diffels JF, Seret ML, Goffeau A, Baret PV. 2006. Heavy metal transporters in Hemiascomycete yeasts. *Biochimie* 88:1639–1649
[14] MacDiarmid CW, Gardner RC. 1998. Overexpression of the *Saccharomyces cerevisiae* magnesium transport system confers resistance to aluminum ion. *Journal of Biological Chemistry* 273:1727–1732
[15] Zhang Q, Zeng G, Chen G, Yan M, Chen A, et al. 2015. The effect of heavy metal-induced oxidative stress on the enzymes in white rot fungus *Phanerochaete chrysosporium*. *Applied Biochemistry and Biotechnology* 175:1281–1293
[16] Stohs SJ, Bagchi D, Hassoun E, Bagchi M. 2001. Oxidative mechanisms in the toxicity of chromium and cadmium ions. *Journal of Environmental Pathology, Toxicology and Oncology* 19:201–213
[17] Vaupotič T, Veranic P, Petrovi č U, Gunde-Cimerman N, Plemenitaš A. 2008. HMG-CoA reductase is regulated by environmental salinity, and its activity is essential for halotolerance in halophilic fungi. *Studies in Mycology* 61:61–66
[18] Wang M, Yang B, Wang H, Zhu Y, Cao X, et al. 2020. Functioning mechanisms of ectomycorrhizal fungi and ectomycorrhiza associated with plant in the tolerance to heavy metal toxicity. *Proceedings of the 2020 The 9th International Conference on Informatics, Environment, Energy and Applications, Amsterdam, The Netherlands, 13–16 March, 2020*. New York, USA: Association for Computing Machinery. pp. 36–40 doi: 10.1145/3386762.3386776
[19] Dey P, Malik A, Singh DK, Haange SB, von Bergen M, et al. 2024. Unveiling fungal strategies: mycoremediation in multi-metal pesticide environment using proteomics. *Scientific Reports* 14:23171
[20] Shishodia SK, Shankar J. 2020. Exploration of mycelial proteins from *Aspergillus terreus* revealed ribosome biogenesis and antioxidant enzymes. *Current Proteomics* 17:433–445
[21] Pang KL, Chiang MW, Guo SY, Shih CY, Dahms HU, et al. 2020. Growth study under combined effects of temperature, pH and salinity and transcriptome analysis revealed adaptations of *Aspergillus terreus* to the extreme conditions at Kueishan Island Hydrothermal Vent Field, Taiwan. *PLoS One* 15:e0233621
[22] Liu Y, Wang L, Feng Y, Liao Q, Lei X, et al. 2024. Untargeted metabolomics approach for the discovery of salinity-related alkaloids in a stony coral-derived fungus *Aspergillus terreus*. *International Journal of Molecular Sciences* 25:10544
[23] Khan MI, Ali N, Jan G, Hamayun M, Jan FG, et al. 2022. Salt stress alleviation in *Triticum aestivum* through primary and secondary metabolites modulation by *Aspergillus terreus* BTK-1. *Frontiers in Plant Science* 13:779623
[24] Krishnaswamy A, Barnes N, Lotlikar NP, Damare SR. 2019. An improved method for protein extraction from minuscule quantities of fungal biomass. *Indian Journal of Microbiology* 59:100–104
[25] Kinter M, Sherman NE. 2000. *Protein Sequencing and Identification Using Tandem Mass Spectrometry*. New Jersey, USA: John Wiley & Sons, Inc. 301 pp. doi: 10.1002/0471721980
[26] Villalba-Villalba AG, González-Méndez B. 2021. Evaluación de la tolerancia de *Aspergillus terreus* a metales tóxicos [Evaluating Aspergillus terreus tolerance to toxic metals]. *Revista Chapingo Serie Ciencias Forestales y del Ambiente* 27:449–464 (in Spanish)
[27] Palanivel TM, Pracejus B, Novo LAB. 2023. Bioremediation of copper using indigenous fungi *Aspergillus* species isolated from an abandoned copper mine soil. *Chemosphere* 314:137688
[28] Soares LW, Bailão AM, de Almeida Soares CM, Bailão MGS. 2020. Zinc at the host–fungus interface: how to uptake the metal? *Journal of Fungi* 6:305
[29] Tang Y, Yang X, Li H, Shuai Y, Chen W, et al. 2023. Uncovering the role of wheat magnesium transporter family genes in abiotic responses. *Frontiers in Plant Science* 14:1078299
[30] Razzaque S, Elias SM, Haque T, Biswas S, Nurnabi Azad Jewel GM, et al. 2019. Gene expression analysis associated with salt stress in a reciprocally crossed rice population. *Scientific Reports* 9:8249
[31] Plemenitaš A. 2021. Sensing and responding to hypersaline conditions and the HOG signal transduction pathway in fungi isolated from hypersaline environments: *Hortaea werneckii* and *Wallemia ichthyophaga*. *Journal of Fungi* 7:988
[32] Song Y, Li F, Ali M, Li X, Zhang X, et al. 2025. Advances in protein kinase regulation of stress responses in fruits and vegetables. *International Journal of Molecular Sciences* 26:768
[33] Almeida-Dalmet S, Litchfield CD, Gillevet P, Baxter BK. 2018. Differential gene expression in response to salinity and temperature in a *Haloarcula* strain from great salt lake, Utah. *Genes* 9:52
[34] Athar HUR, Zulfiqar F, Moosa A, Ashraf M, Zafar ZU, et al. 2022. Salt stress proteins in plants: an overview. *Frontiers in Plant Science* 13:999058
[35] Lopez-Ortiz C, Peña-Garcia Y, Natarajan P, Bhandari M, Abburi V, et al. 2020. The ankyrin repeat gene family in *Capsicum* spp.: genome-wide survey, characterization and gene expression profile. *Scientific Reports* 10:4044
[36] González-Guerrero M, Escudero V, Saéz Á, Tejada-Jiménez M. 2016. Transition metal transport in plants and associated endosymbionts: arbuscular mycorrhizal fungi and rhizobia. *Frontiers in Plant Science* 7:1088
[37] Sun GL, Reynolds EE, Belcher AM. 2019. Designing yeast as plant-like hyperaccumulators for heavy metals. *Nature Communications* 10:5080
[38] Murugesan A, Kumar A, Gunasekar A, Arumugam I, Eswaran K, et al. 2016. Hsp70 and theta subunit of T complex protein, a response to salt stress in the halophyte *Sesuvium portulacastrum*. *Journal of Bioinformatics and Proteomics Review* 2:1–9
[39] Eisenberg E, Levanon EY. 2003. Human housekeeping genes are compact. *Trends in Genetics* 19:362–365
[40] Tao Y, Van Peer AF, Huang Q, Shao Y, Zhang L, et al. 2016. Identification of novel and robust internal control genes from *Volvariella volvacea* that are suitable for RT-qPCR in filamentous fungi. *Scientific Reports* 6:29236
[41] Waxman S, Wurmbach E. 2007. De-regulation of common housekeeping genes in hepatocellular carcinoma. *BMC Genomics* 8:243
[42] Chang YC, Ding Y, Dong L, Zhu LJ, Jensen RV, et al. 2018. Differential expression patterns of housekeeping genes increase diagnostic and prognostic value in lung cancer. *PeerJ* 6:e4719
[43] Irie N, Warita K, Tashiro J, Zhou Y, Ishikawa T, et al. 2023. Expression of housekeeping genes varies depending on mevalonate pathway inhibition in cancer cells. *Heliyon* 9:e18017
[44] Casas AI, Hassan AA, Manz Q, Wiwie C, Kleikers P, et al. 2022. Un-biased housekeeping gene panel selection for high-validity gene expression analysis. *Scientific Reports* 12:12324